nature biotechnology

Real-time imaging of hepatitis C virus infection using a fluorescent cell-based reporter system

Christopher T Jones[1], Maria Teresa Catanese[1], Lok Man J Law[1], Salman R Khetani[2,5], Andrew J Syder[1,5], Alexander Ploss[1], Thomas S Oh[1], John W Schoggins[1], Margaret R MacDonald[1], Sangeeta N Bhatia[2–4] & Charles M Rice[1]

Hepatitis C virus (HCV), which infects 2–3% of the world population, is a causative agent of chronic hepatitis and the leading indication for liver transplantation[1]. The ability to propagate HCV in cell culture (HCVcc) is a relatively recent breakthrough and a key tool in the quest for specific antiviral therapeutics. Monitoring HCV infection in culture generally involves bulk population assays, use of genetically modified viruses and/or terminal processing of potentially precious samples. Here we develop a cell-based fluorescent reporter system that allows sensitive distinction of individual HCV-infected cells in live or fixed samples. We demonstrate use of this technology for several previously intractable applications, including live-cell imaging of viral propagation and host response, as well as visualizing infection of primary hepatocyte cultures. Integration of this reporter with modern image-based analysis methods could open new doors for HCV research.

For over two decades, advances in HCV assay systems have been hard-won. Methodologies have ranged from adapted selectable genomes and detection methods that require fixation or cell lysis, such as immunostaining and quantitative RT PCR, to the use of infectious reporter viruses[2,3]. Broadening the scope of HCV research, however, will require versatile new assays that allow sensitive single-cell analysis of infection events using unmodified viral genomes.

To construct a cellular marker of HCV infection, we adapted a known substrate of the HCV NS3-4A protease[4–6], the mitochondrially tethered interferon (IFN)-β promoter stimulator protein 1 (IPS-1; ref. 7), also termed MAVS[8], VISA[9] or Cardif[4]. The C-terminal region of IPS-1, encompassing the NS3-4A recognition site and a mitochondrial targeting sequence, was fused to green fluorescent protein (EGFP-IPS, **Fig. 1a**) or to the red fluorescent proteins (RFPs) mCherry or TagRFP. We also introduced an SV40 nuclear localization sequence (NLS) between the RFP variant and IPS-1 segment (RFP-NLS-IPS, **Fig. 1a**). Human hepatoma (Huh-7.5) cells stably transduced with lentiviruses encoding EGFP-IPS or RFP-NLS-IPS exhibited punctate fluorescence consistent with mitochondrial localization of the reporter, which was confirmed by colocalization with native IPS-1 (**Fig. 1b**).

We determined the reporter phenotype of the EGFP-IPS or RFP-NLS-IPS constructs in the presence of NS3-4A by transduction into Huh-7.5 cells stably expressing an autonomously replicating HCV subgenome[10] (JFH-1 strain, SG-JFH). Replicon-harboring cells expressing EGFP-IPS showed diffuse fluorescence, whereas an NS3-4A cleavage–resistant form[11] of the reporter (EGFP-IPS(C508Y); **Fig. 1c**) exhibited a punctate pattern. Similarly, replicon-containing Huh-7.5 cells expressing RFP-NLS-IPS, but not RFP-NLS-IPS(C508Y), showed nuclear translocation of fluorescence (**Fig. 1c**). Both reporters displayed a punctate pattern in the absence of the HCV replicon (**Fig. 1c**). These results indicate that cleavage of EGFP-IPS and RFP-NLS-IPS are dependent on an intact NS3-4A recognition site and that HCV-dependent fluorescence relocalization (HDFR) can be used as a marker of viral replication.

HCV exists as multiple genotypes, which exhibit extensive sequence divergence as well as differences in pathogenesis and treatment susceptibility[12]. Evasion of the innate immune response by cleavage of native IPS-1, however, is likely to be a conserved feature of HCV infection. In addition to JFH-1 (genotype 2a), Huh-7.5 cells harboring H77 (genotype 1a) or Con1 (genotype 1b) subgenomes[10] were transduced with EGFP-IPS or EGFP-IPS(C508Y). Regardless of the HCV strain, EGFP-IPS transduction resulted in diffuse fluorescence, and EGFP-IPS(C508Y) expression led to punctate EGFP (**Fig. 1c**). Whereas the lack of replicon systems for other genotypes precludes comprehensive analysis, these results indicate that cleavage of EGFP-IPS can be used as a marker of several diverse HCV strains. In contrast, replication of other positive-strand RNA viruses, such as yellow fever virus or Venezuelan equine encephalitis virus, did not lead to fluorescence relocalization (**Supplementary Fig. 1a**). These results suggest that the HDFR reporter system achieves a high level of HCV specificity combined with genotype independence.

Although replicon-containing cells constitutively express the viral proteins, monitoring authentic virus infection is important for analyses of HCV biology and therapeutic inhibition. To determine the ability of HDFR to detect infection, we inoculated Huh-7.5 cells expressing RFP-NLS-IPS with an HCVcc reporter virus expressing secreted *Gaussia* luciferase, Jc1FLAG2(p7-nsGluc2A)[13], followed by

[1]Center for the Study of Hepatitis C, Laboratory of Virology and Infectious Disease, The Rockefeller University, New York, New York, USA. [2]Division of Health Sciences and Technology, Department of Electrical Engineering and Computer Science, Massachusetts Institute of Technology, Cambridge, Massachusetts, USA. [3]Howard Hughes Medical Institute, [4]Division of Medicine, Brigham & Women's Hospital, Boston, Massachusetts, USA. [5]Present addresses: Hepregen Corporation, Medford, Massachusetts, USA (S.R.K.) and iTherX Pharmaceuticals, San Diego, California, USA (A.J.S.). Correspondence should be addressed to C.M.R. (ricec@rockefeller.edu).

Received 17 August 2009; accepted 4 January 2010; published online 31 January 2010; doi:10.1038/nbt.1604

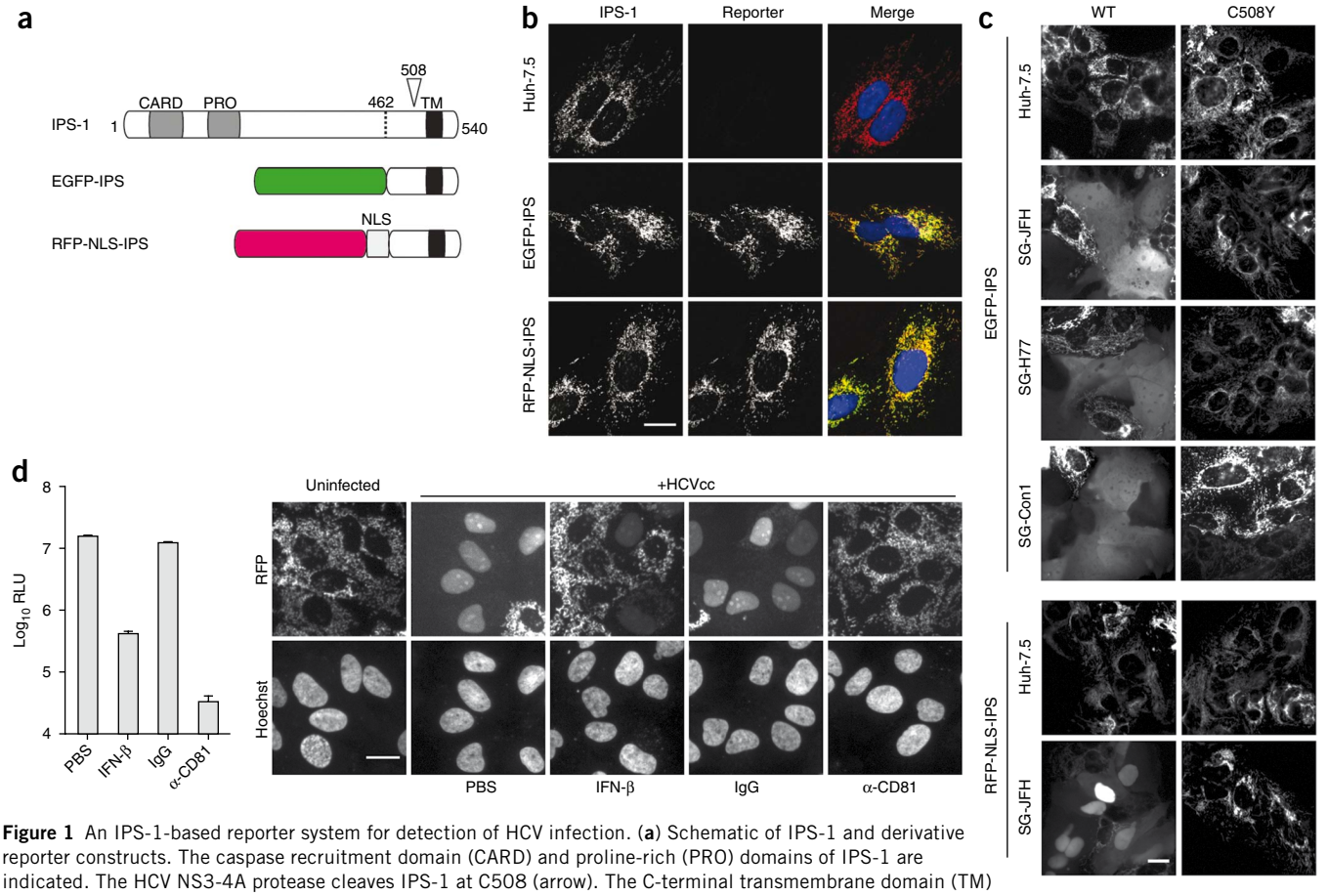

Figure 1 An IPS-1-based reporter system for detection of HCV infection. (**a**) Schematic of IPS-1 and derivative reporter constructs. The caspase recruitment domain (CARD) and proline-rich (PRO) domains of IPS-1 are indicated. The HCV NS3-4A protease cleaves IPS-1 at C508 (arrow). The C-terminal transmembrane domain (TM) directs IPS-1 to the outer membrane of mitochondria. EGFP-IPS encodes EGFP fused to residues 462–540 of IPS-1. RFP-NLS-IPS encodes a red fluorescent protein (mCherry or TagRFP) and an SV40 nuclear localization signal (NLS, PKKKRKVG) fused to residues 462–540 of IPS-1. (**b**) EGFP-IPS and RFP-NLS-IPS localize to mitochondria in Huh-7.5 cells. Native IPS-1, detected by immunofluorescent staining (IPS-1), and EGFP or RFP autofluorescence (Reporter) were visualized in untransduced (Huh-7.5) or transduced (EGFP-IPS or RFP-NLS-IPS) cells by confocal microscopy. Merge images also depict Hoechst nuclear dye (blue). (**c**) EGFP-IPS and RFP-NLS-IPS relocalize in response to HCV replication. Huh-7.5 cell lines harboring subgenomic (SG) neomycin-selectable replicons were transduced with lentiviruses expressing wild type (WT) or mutant (C508Y) EGFP-IPS or RFP-NLS-IPS. H77, genotype 1a; Con1, genotype 1b; JFH-1, genotype 2a. Wide-field fluorescence images of unfixed cells are shown. (**d**) RFP-NLS-IPS relocalizes in HCV-infected cells. Huh-7.5 cells expressing RFP-NLS-IPS were infected with secreted *Gaussia* luciferase HCVcc reporter virus, Jc1FLAG2(p7-nsGluc2A), in the presence of PBS, IFN-β, blocking antibody (α-CD81) or isotype control (IgG). Luciferase activity in the culture supernatants (left) and reporter (RFP) or nuclear dye (Hoechst) fluorescence (right) were monitored at 48 h post-infection. Wide-field fluorescence images of fixed cells are shown. Scale bars, 20 μm. RLU, relative light units.

incubation for 48 h. Uninfected cells showed punctate fluorescence, whereas HCV-infected cultures displayed a distinct nuclear signal (**Fig. 1d**). Inoculation in the presence of IFN-β largely abolished the fluorescence translocation phenotype. Similarly, cells infected in conjunction with a monoclonal antibody targeting a known HCV entry factor (α-CD81) did not show nuclear fluorescence. Detection of *Gaussia* luciferase in the culture supernatants yielded corresponding results (**Fig. 1d**). Staining for viral replicase protein NS5A in infected EGFP-IPS–expressing cells supported the correlation between fluorescence relocalization and HCV replication at the single-cell level (**Supplementary Fig. 1b**).

Monitoring infection by fluorescence relocalization does not require cells to be fixed, lysed or processed. These advantages suggested the possibility of real-time visualization of HCV infection in live cells. Huh-7.5 cells expressing RFP-NLS-IPS and a constitutive mitochondrial marker (EGFP-cytochrome *c* oxidase subunit VIII fusion protein; mito-EGFP) were inoculated with Jc1FLAG2 (p7-nsGluc2A) and monitored by live-cell microscopy beginning at 6 h post-infection (**Fig. 2a**,**b**; DMSO). Translocation of RFP-NLS to the nucleus could be detected as early as 10–12 h post-inoculation, with complete cleavage by 16–18 h (**Fig. 1b** and **Supplementary Video 1a**). In contrast, cells infected in the presence of a viral RNA-dependent RNA polymerase inhibitor (2′CMA)[14] showed very limited nuclear fluorescence (**Fig. 2b** and **Supplementary Video 1b**). We then investigated whether drug treatment of cells with established HCV infection could lead to observable reconstitution of mitochondrially localized fluorescence. RFP-NLS-IPS reporter cells were infected with Jc1FLAG2(p7-nsGluc2A) for 24 h before treatment with VX-950, an inhibitor of the NS3-4A[15] protease, or DMSO as a vehicle control and imaged for an additional 24 h (**Fig. 2a**,**c**). Over the time course of the experiment, RFP-NLS-IPS localization in DMSO cells remained unchanged, whereas steady reconstitution of punctate fluorescence was seen in the majority of infected cells treated with the protease inhibitor. These results indicate that the reporter system can be used to visually monitor NS3-4A inhibition in real time (**Supplementary Video 1c**,**d**).

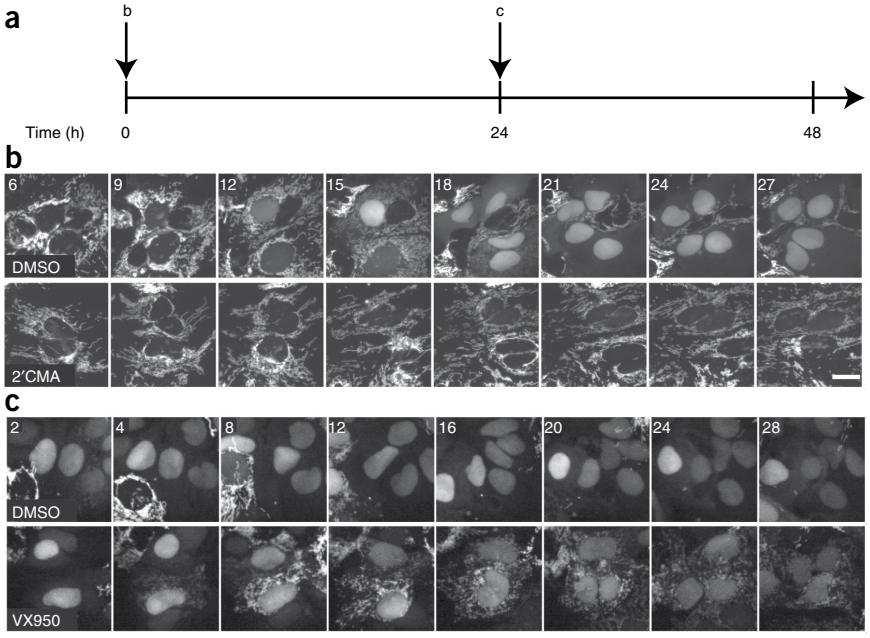

Figure 2 Time-lapse live-cell imaging of HCVcc infection. (**a**) Schematic of live-cell imaging time course. Huh-7.5 cells stably expressing RFP-NLS-IPS and a mitochondrially targeted EGFP-cytochrome *c* oxidase subunit VIII fusion protein (mito-EGFP) were infected with HCVcc reporter virus, Jc1FLAG2(p7-nsGluc2A) (time = 0 h). (**b**) Cells were infected in the presence of DMSO or HCV RNA-dependent RNA polymerase inhibitor 2′CMA. (**c**) Cells were infected for 24 h before removal of the inoculum and addition of imaging medium containing DMSO or the NS3-4A protease inhibitor VX-950. Images were captured every 30 min starting at 6 h (**b**) or 24.5 h (**c**) post-infection. RFP fluorescence is shown in grayscale. Time (h) from the start of infection (**b**) or drug addition (**c**) are indicated. Scale bar, 20 µm. See **Supplementary Video 1a–d** for the full time course.

The availability of spectrally distinct HDFR reporters (EGFP-IPS and RFP-NLS-IPS) suggested the possibility of discerning infection in two separate cell populations simultaneously. We applied this advantage to visualize the recently described phenomenon of CD81-independent HCV infection. Circulating HCV enters hepatocytes through a complex pathway involving multiple co-receptors. CD81, SCARB1 and two tight-junction proteins, CLDN1 and OCLN, have been shown to be essential for this process[16–19]. Recent reports, however, suggest a second, CD81-independent route of virus entry, which may entail particle transfer through close cell-cell contacts[20,21]. This transmission mode may be highly biologically relevant in the context of chronic infection, and the development of inhibitors targeting this entry pathway necessitates a reliable method of detection. To monitor routes of HCV spread, we employed cells expressing RFP-NLS-IPS and EGFP-IPS as producer and target populations, respectively. EGFP-IPS target cells were engineered to stably express a short hairpin (sh)RNA targeting CD81 (EGFP-IPS/CD81$^-$) or an irrelevant sequence (EGFP-IPS/IRR), and tested for permissiveness to cell-free virus using an adapted HCVcc (J6/JFH clone 2), which exhibits superior titers to J6/JFH[22]. Cells expressing CD81 shRNA had undetectable levels of CD81 protein (**Supplementary Fig. 2a**). At 48 h post-infection, the majority of EGFP-IPS/IRR cells exhibited diffuse EGFP, whereas EGFP-IPS/CD81$^-$ cells were largely nonpermissive (**Fig. 3a**). Fluorescence-activated cell sorting (FACS) analysis of fixed samples stained with an NS5A antibody supported these observations, indicating that <1% of EGFP-IPS/CD81$^-$ cells were infected, compared to ~80% of the EGFP-IPS/IRR targets (**Supplementary Fig. 2**). To investigate HCV transmission in a mixed cell population, we pre-infected RFP-NLS-IPS cells for 36 h before co-culturing with EGFP-IPS/IRR or EGFP-IPS/CD81$^-$ target cells. Mixing uninfected RFP-NLS-IPS cells with either target population did not result in EGFP relocalization. In contrast, the majority of EGFP-IPS/IRR cells exhibited diffuse fluorescence upon co-culture with infected producers, presumably as a result of both CD81-dependent and CD81-independent infection routes. Culture of infected producer cells with EGFP-IPS/CD81$^-$ targets also led to EGFP-IPS cleavage, correlating with CD81-independent infection of 10–15% of cells (**Fig. 3a** and **Supplementary Fig. 2**). Use of the HDFR system in a mixed population can therefore provide a rapid visual assay for CD81-independent HCV spread.

In addition to exploiting a number of cellular factors during virus uptake, HCV affects host pathways during replication and pathogenesis. The ability to correlate infection with altered cell biology on a single-cell level would be invaluable to detecting virus-induced phenotypes. We therefore examined whether HDFR could be multiplexed with fluorescent markers of host processes. Stress pathways are charged with protecting the cell against various environmental insults, including heat shock, oxidative stress and virus infection. In response to stress, phosphorylation of translation factor eIF2α leads to the appearance of cytoplasmic stress granules, in which mRNAs are triaged and translation is stalled (reviewed in ref. 23). Not surprisingly, many viruses have evolved mechanisms to modulate the stress response and subvert translational suppression (reviewed in ref. 24); the effect of HCV on stress granule formation is unknown. We examined the stress response in Huh-7 cells expressing RFP-NLS-IPS and EGFP-tagged Ras-Gap-SH3 domain binding protein (EGFP-G3BP), a marker of stress granule formation[25]. Transduced cells were infected with Jc1FLAG2(p7-nsGluc2A) and subsequently monitored by live cell imaging; HCV replication was readily observed starting at 14–16 h post-infection. EGFP-G3BP exhibited a cytoplasmic distribution until ~30 h post-infection, when stress granule formation commenced in a fraction of HCV-positive cells. Interestingly, stress granules often appeared to be transient and, in some cases, formed and dissolved multiple times within a single cell (**Fig. 3b**). Stress granule formation was not observed in neighboring uninfected cells, nor in infected cultures treated with 2′CMA (**Supplementary Video 2a–c**), suggesting a dependence on HCV replication. Although the mechanisms underlying this phenomenon are still obscure, these observations support the utility of single-cell analysis and reporter multiplexing for discovery and dissection of virus-host interactions.

Although we have demonstrated that HDFR can be used to detect infection of highly permissive hepatoma cell lines, we also sought to monitor HCV uptake by primary human hepatocytes. Primary cells are arguably the most relevant culture system in which to study HCV biology, but they have traditionally posed substantial challenges. Primary hepatocytes show low permissiveness for both viral entry and RNA replication, leading to poor expression of HCV-specific antigens, and making standard immunofluorescence techniques unreliable for visualizing infection. We reasoned that the sensitivity of HDFR might circumvent these

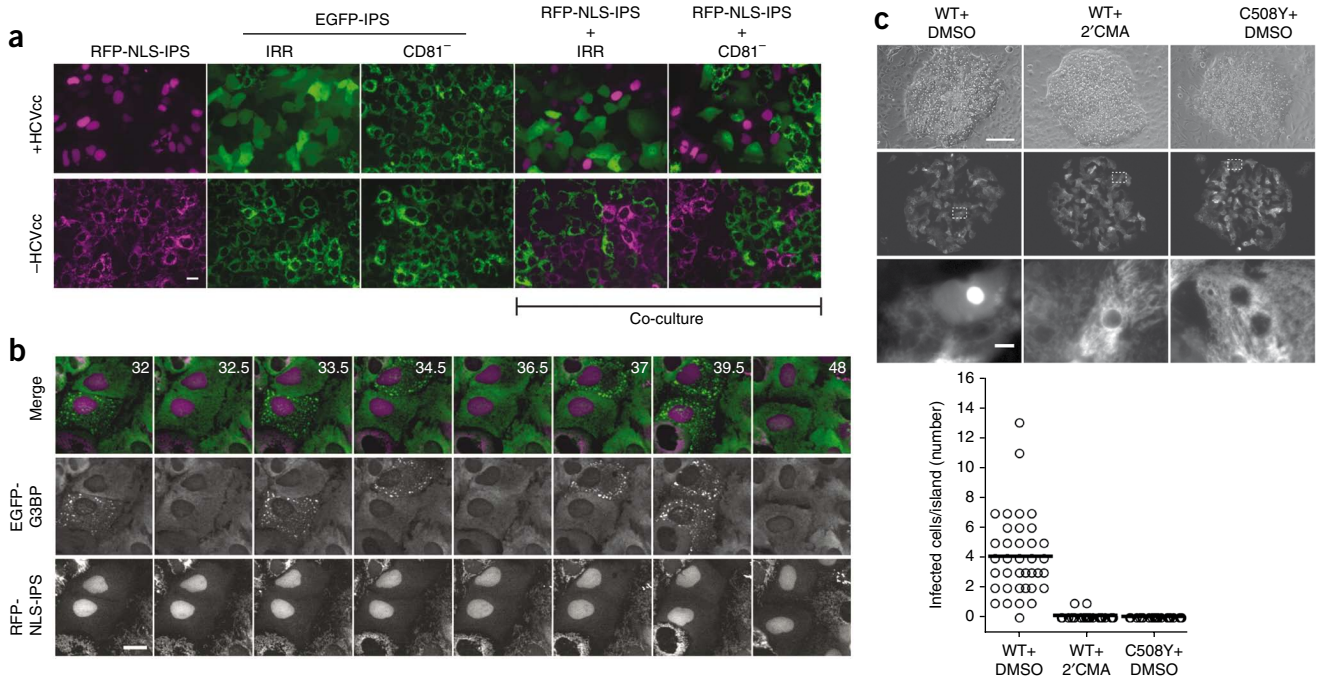

Figure 3 Use of the IPS-1-based reporter to expand HCVcc culture systems. (**a**) Co-culture of spectrally distinct HCV reporter cell lines for visualizing CD81-independent infection. Wide-field fluorescence images of unfixed mono- and co-cultures of Huh-7.5 cell lines expressing RFP-NLS-IPS or EGFP-IPS in the presence (+HCVcc) or absence (–HCVcc) of J6/JFH clone 2. EGFP-IPS cells stably express shRNA targeting CD81 (CD81⁻) or an irrelevant sequence (IRR). Monocultures were infected for 72 h before imaging. In co-culture experiments, RFP-NLS-IPS cells were infected with HCVcc for 36 h before mixing with uninfected EGFP-IPS/IRR or EGFP-IPS/CD81⁻ cells. Co-cultures were incubated for an additional 48 h before imaging. (**b**) Multiplexing the HCV reporter with a marker of the stress response. An Huh-7 cell line expressing RFP-NLS-IPS and an EGFP-tagged stress granule marker (EGFP-G3BP) was infected with Jc1FLAG2(p7-nsGluc2A). Live-cell imaging was initiated at 6 h post-infection with images captured every 30 min. Montage shows selected time points beginning at 32 h post-infection; times (h) from the start of infection are indicated. See **Supplementary Videos 2a–c**. (**c**) Visualization of HCVcc infection in primary hepatocytes. Primary human hepatocytes maintained as MPCCs were transduced with lentiviruses expressing wild type (WT) or mutant (C508Y) RFP-NLS-IPS. At 24 h post-transduction, MPCCs were infected with Jc1FLAG2(p7-nsGluc2A). After 12 h, virus was removed and MPCC medium containing DMSO or 2′CMA was added. Unfixed MPCCs were imaged by wide-field fluorescence microscopy at 48 h post-infection. Representative phase contrast (top row) and corresponding RFP fluorescence images (middle row) are shown. Enlarged fluorescence images (bottom row) correspond to area denoted by white dotted box (middle row). The number of cells per MPCC island exhibiting nuclear RFP at 48 h post-infection is plotted for each condition. For WT RFP-NLS-IPS+DMSO, $n = 40$; WT RFP-NLS-IPS+2′CMA, $n = 30$; C508Y RFP-NLS-IPS+DMSO, $n = 35$. Bar, mean number of positive cells/island. Scale bars, 20 μm (**a** and **b**), 200 μm (**c**, top row), 10 μm (**c**, lower row).

difficulties, and explored its use for detecting HCV infection in the recently developed micropattern co-culture (MPCC) system[26]. MPCCs consist of primary adult human hepatocytes seeded on islands of collagen and surrounded by mouse fibroblast 'feeder' cells. These conditions allow hepatocytes to be maintained for extended periods without the rapid decline in cellular functions seen in conventional monocultures or random co-cultures[27]. To visualize HCV infection in MPCC hepatocytes, we transduced cultures with RFP-NLS-IPS or RFP-NLS-IPS(C508Y) and infected them 48 h later with Jc1FLAG2(p7-nsGluc2A), allowing MPCC infection to be monitored in parallel by *Gaussia* luciferase secretion[28] (**Supplementary Fig. 3**). MPCC islands were examined by live cell microscopy and the cells per island exhibiting nuclear RFP were enumerated (**Fig. 3c**). In cultures transduced with RFP-NLS-IPS followed by DMSO treatment, ~98% of the islands observed contained cells with nuclear RFP, averaging four cells/island. In the RFP-NLS-IPS population treated with 2′CMA, only 6% of islands exhibited infected cells, corresponding to an average of 0.06 cells/island. Cells transduced with RFP-NLS-IPS(C508Y) did not show nuclear RFP in any of the islands examined (**Fig. 3c**). These results indicate that infection of primary hepatocytes can be readily detected using the HDFR system. To our knowledge, visualization of HCV infection in live primary hepatocytes has not been demonstrated previously.

Although systems for tracking HCV replication in culture have expanded rapidly in recent years, robust detection methods applicable to imaging of individual live cells have not been available. We describe a sensitive HCV reporter that allows easy distinction of infected and uninfected cells in live or fixed cultures by standard fluorescence microscopy. The robust signal of the reporter system derives from the efficiency of NS3-4A cleavage and the constitutive high-level expression of the substrate; nuclear translocation increases visualization, as the reporter becomes concentrated in a region with low autofluorescence, a particular advantage when working with hepatocytes. Although reporter cleavage does not occur in the absence of an active protease, transient signal may be expected in the presence of a polymerase inhibitor—this high sensitivity may have to be factored in as 'background' for some applications. The HDFR system does not require genetic modification of the viral genome and showed efficient detection of all HCV genotypes tested. This raises the possibility of using the reporter to identify novel infectious isolates directly from patient samples, potentially expanding the HCVcc system beyond the currently available genotype 2a strain. Coaxing

HCVcc to infect biologically relevant primary cell types may also be key to understanding authentic viral processes and patient-specific responses. The low level of replication observed in these cultures may reflect heterogeneity between individual cells or viral genomes, and underscores the value of single-cell analysis in dissecting the often subtle or variable phenotypes associated with chronic infection. Combining HDFR-based visualization with laser capture microscopy and analysis of neighboring infected and uninfected cells could begin to unravel the determinants of pathogenesis or virus control. The value of single-cell analysis was further illustrated by multiplexing HCV detection with a fluorescent marker of cellular stress, allowing direct visual correlation of viral and host events. Recent advances in automated microscopy and 'high-content' screening have made a large number of cellular phenotypes, including drug toxicity profiles, accessible to interrogation in a multiparametric format (reviewed in ref. 29). Addition of a robust fluorescent translocation assay requiring minimal sample processing has the potential to integrate HCV research into this burgeoning field. We anticipate that the ability of HDFR to increase the flexibility and diversity of HCV culture systems will be important for basic virology and antiviral drug development.

METHODS

Methods and any associated references are available in the online version of the paper at http://www.nature.com/naturebiotechnology/.

Note: Supplementary information is available on the Nature Biotechnology website.

ACKNOWLEDGMENTS

We acknowledge the expert support of The Rockefeller University Bioimaging Core Facility, with special thanks to A. North, S. Galdeen and S. Bhuvanendran. We thank The Rockefeller University Flow Cytometry Resource Center, supported by the Empire State Stem Cell Fund through NY State Department of Health (NYSDOH) contract no. C023046; opinions expressed here are solely those of the authors and do not necessarily reflect those of the Empire State Stem Cell Fund, the NYSDOH, or the State of NY. We are grateful to C. Stoyanov (The Rockefeller University) for YF17D(5′C25Venus2AUbi), J. Tazi for G3BP (Institut de Génétique Moléculaire de Montpellier) and I. Frolov (UTMB) for Venezuelan equine encephalitis virus-EGFP. We thank M. Holz, A. Forest, M. Panis and A. Webson for laboratory support and C. Murray for critical reading of the manuscript. This work was supported by Public Health Service grants R01 AI075099 (C.M.R.) and R01 DK56966 (S.N.B.). This work was also funded by the Office of the Director/National Institutes of Health (NIH) through the NIH Roadmap for Medical Research, Grant 1 R01 DK085713-01 (C.M.R. and S.N.B.). Information on this Roadmap Transformative R01 Program can be found at http://grants.nih.gov/grants/guide/rfa-files/RFA-RM-08-029.html. Additional funding was provided by the Greenberg Medical Research Institute and the Starr Foundation (C.M.R.). S.N.B. is an Howard Hughes Medical Investigator investigator. C.T.J. was supported by National Research Service Award DK081193; M.T.C. was supported by a Women & Science Fellowship; L.M.J.L. is supported by a Natural Sciences and Engineering Research Council of Canada fellowship. A.P. is a recipient of a Kimberly Lawrence-Netter cancer research discovery fund award.

AUTHOR CONTRIBUTIONS

C.T.J. and C.M.R. designed the project, analyzed results and wrote the manuscript. C.T.J., M.T.C., L.M.J.L., A.J.S., S.R.K., T.S.O., A.P. and J.W.S. performed the experimental work. S.R.K., J.W.S., T.S.O., M.R.M. and S.N.B. contributed reagents and technical expertise.

COMPETING INTERESTS STATEMENT

The authors declare competing financial interests: details accompany the full-text HTML version of the paper at http://www.nature.com/naturebiotechnology/.

Published online at http://www.nature.com/naturebiotechnology/.
Reprints and permissions information is available online at http://npg.nature.com/reprintsandpermissions/.

1. Shepard, C.W., Finelli, L. & Alter, M.J. Global epidemiology of hepatitis C virus infection. *Lancet Infect. Dis.* **5**, 558–567 (2005).
2. Bartenschlager, R. & Sparacio, S. Hepatitis C virus molecular clones and their replication capacity in vivo and in cell culture. *Virus Res.* **127**, 195–207 (2007).
3. Bartenschlager, R. Hepatitis C virus molecular clones: from cDNA to infectious virus particles in cell culture. *Curr. Opin. Microbiol.* **9**, 416–422 (2006).
4. Meylan, E. *et al.* Cardif is an adaptor protein in the RIG-I antiviral pathway and is targeted by hepatitis C virus. *Nature* **437**, 1167–1172 (2005).
5. Foy, E. *et al.* Control of antiviral defenses through hepatitis C virus disruption of retinoic acid-inducible gene-I signaling. *Proc. Natl. Acad. Sci. USA* **102**, 2986–2991 (2005).
6. Li, X.D., Sun, L., Seth, R.B., Pineda, G. & Chen, Z.J. Hepatitis C virus protease NS3/4A cleaves mitochondrial antiviral signaling protein off the mitochondria to evade innate immunity. *Proc. Natl. Acad. Sci. USA* **102**, 17717–17722 (2005).
7. Kawai, T. *et al.* IPS-1, an adaptor triggering RIG-I- and Mda5-mediated type I interferon induction. *Nat. Immunol.* **6**, 981–988 (2005).
8. Seth, R.B., Sun, L., Ea, C.K. & Chen, Z.J. Identification and characterization of MAVS, a mitochondrial antiviral signaling protein that activates NF-kappaB and IRF 3. *Cell* **122**, 669–682 (2005).
9. Xu, L.G. *et al.* VISA is an adapter protein required for virus-triggered IFN-beta signaling. *Mol. Cell* **19**, 727–740 (2005).
10. Tscherne, D.M. *et al.* Superinfection exclusion in cells infected with hepatitis C virus. *J. Virol.* **81**, 3693–3703 (2007).
11. Loo, Y.M. *et al.* Viral and therapeutic control of IFN-beta promoter stimulator 1 during hepatitis C virus infection. *Proc. Natl. Acad. Sci. USA* **103**, 6001–6006 (2006).
12. Simmonds, P. Genetic diversity and evolution of hepatitis C virus-15 years on. *J. Gen. Virol.* **85**, 3173–3188 (2004).
13. Marukian, S. *et al.* Cell culture-produced hepatitis C virus does not infect peripheral blood mononuclear cells. *Hepatology* **48**, 1843–1850 (2008).
14. Carroll, S.S. *et al.* Inhibition of hepatitis C virus RNA replication by 2′-modified nucleoside analogs. *J. Biol. Chem.* **278**, 11979–11984 (2003).
15. Lin, K., Perni, R.B., Kwong, A.D. & Lin, C. VX-950, a novel hepatitis C virus (HCV) NS3–4A protease inhibitor, exhibits potent antiviral activities in HCV replicon cells. *Antimicrob. Agents Chemother.* **50**, 1813–1822 (2006).
16. Pileri, P. *et al.* Binding of hepatitis C virus to CD81. *Science* **282**, 938–941 (1998).
17. Scarselli, E. *et al.* The human scavenger receptor class B type I is a novel candidate receptor for the hepatitis C virus. *EMBO J.* **21**, 5017–5025 (2002).
18. Evans, M.J. *et al.* Claudin-1 is a hepatitis C virus co-receptor required for a late step in entry. *Nature* **446**, 801–805 (2007).
19. Ploss, A. *et al.* Human occludin is a hepatitis C virus entry factor required for infection of mouse cells. *Nature* **457**, 882–886 (2009).
20. Timpe, J.M. *et al.* Hepatitis C virus cell-cell transmission in hepatoma cells in the presence of neutralizing antibodies. *Hepatology* **47**, 17–24 (2008).
21. Witteveldt, J. *et al.* CD81 is dispensable for hepatitis C virus cell-to-cell transmission in hepatoma cells. *J. Gen. Virol.* **90**, 48–58 (2009).
22. Diamond, D.L. *et al.* Temporal proteome and lipidome profiles reveal HCV-associated reprogramming of hepatocellular metabolism and bioenergetics. *PLoS Pathog.* **6**, e1000719 (2010).
23. Anderson, P. & Kedersha, N. RNA granules. *J. Cell Biol.* **172**, 803–808 (2006).
24. Schutz, S. & Sarnow, P. How viruses avoid stress. *Cell Host Microbe* **2**, 284–285 (2007).
25. Tourriere, H. *et al.* The RasGAP-associated endoribonuclease G3BP assembles stress granules. *J. Cell Biol.* **160**, 823–831 (2003).
26. Khetani, S.R. & Bhatia, S.N. Microscale culture of human liver cells for drug development. *Nat. Biotechnol.* **26**, 120–126 (2008).
27. Bhatia, S.N., Balis, U.J., Yarmush, M.L. & Toner, M. Effect of cell-cell interactions in preservation of cellular phenotype: cocultivation of hepatocytes and nonparenchymal cells. *FASEB J.* **13**, 1883–1900 (1999).
28. Ploss, A. *et al.* Persistent hepatitis C virus infection in microscale primary human hepatocyte cultures. *Proc. Natl. Acad. Sci. USA* (in the press).
29. Wollman, R. & Stuurman, N. High throughput microscopy: from raw images to discoveries. *J. Cell Sci.* **120**, 3715–3722 (2007).

ONLINE METHODS

Cell culture. Huh-7 and Huh-7.5 cells were cultured at 37 °C, 5% CO_2 in Dulbecco's Modified Eagle Medium (DMEM, Invitrogen) containing 10% FBS and 0.1 mM nonessential amino acids (NEAA) (complete media), unless otherwise noted. For time-lapse imaging, cells were maintained in CO_2-independent media (Invitrogen) containing 10% FBS, 0.1 mM NEAA, 1 mM sodium pyruvate and 2 mM L-glutamine (imaging media). Huh-7.5 cell lines harboring selectable subgenomic replicons[10] were grown in complete media containing 0.5 mg/ml G418. Huh-7.5 cells stably expressing the pLenti-3′-U6-EC-EP7 vector encoding an shRNA against CD81 (nt 268-288, cDNA numbering) or a predicted nontargeting sequence (IRR) have been previously described[21] and were grown in complete media containing 6 μg/ml blasticidin. MPCC cultures were generated as previously described[26] and maintained in high glucose DMEM, 10% FBS, 0.5 U/ml insulin, 7 ng/ml glucagon, 7.5 μg/ml hydrocortisone and 1% penicillin-streptomycin. For HCV inhibition, culture media was supplemented with 0.2% DMSO, 14 mM 2′CMA, 24 mM VX-950, or 1,000 U/ml IFN-β (Peprotech). For neutralization experiments, HCVcc infections were performed in the presence of 10 μg/ml antibody directed against CD81 (BD Biosciences) or an isotype control (IgG1κ, BD Biosciences).

Virus stocks. Jc1[30] and Jc1FLAG2(p7-nsGluc2A)[13] are fully infectious HCVcc viruses that have been previously described. J6/JFH clone 2 is a passaged derivative of J6/JFH[31] that contains a number of adaptive mutations that increase infectious titers[22]. Bi-Ypet-Jc1FLAG2 is a bicistronic reporter virus in which the HCV IRES drives expression of Ypet, an EGFP variant with enhanced brightness, in the first cistron; the EMCV IRES drives expression of the second cistron, which encodes the Jc1 polyprotein with a FLAG epitope at the N terminus of E2. YF17D(5′C25Venus2AUbi) is a monocistronic yellow fever reporter virus (kindly provided by C. Stoyanov, The Rockefeller University) encoding the Venus fluorescent protein, a yellow-shifted variant of EGFP. Venezuelan equine encephalitis virus-EGFP (kindly provided by I. Frolov, UTMB) is a double subgenomic EGFP reporter virus derived from the TC83 vaccine strain of Venezuelan equine encephalitis. Virus stocks were generated by electroporation of *in vitro* transcribed RNAs into the appropriate cell lines, as described previously[31–33].

Plasmid constructs. Constructs were created by standard methods; plasmid and primer sequences are available upon request. IPS-1–based reporters and subcellular localization markers were constructed in a lentivirus backbone derived from TRIP-EGFP[34]. Residues 462–540 of IPS-1 (IPS) were obtained by PCR from a human hepatocyte cDNA library (Ambion) and inserted into the BsrGI/XhoI sites of TRIP-EGFP to generate TRIP-EGFP-IPS. IPS-1 mutation C508Y was generated by overlap PCR mutagenesis. TRIP-mCherry and TRIP-TagRFP were used to construct TRIP-RFP-NLS-IPS plasmids. TRIP-mCherry was derived from the TRIP-mCherry-CLDN1 plasmid[18]. TagRFP sequence was obtained from pTagRFP-C (Evrogen). TRIP-RFP-NLS-IPS plasmids encode the SV40 nuclear localization signal (NLS, PKKKRKVG) and IPS fused to the C terminus of RFP. TRIP-mito-EGFP, encodes the mitochondrial targeting sequence of human cytochrome *c* oxidase subunit VIII fused to the N terminus of EGFP. TRIP-EGFP-G3BP encodes the Ras-Gap-SH3 domain binding protein (G3BP, kindly provided by J. Tazi[25]) fused to the C terminus of EGFP.

Generation of lentivirus pseudoparticles and transductions. Pseudoparticles (pp) were generated by co-transfection of 293T cells with TRIP provirus, HIV gag-pol, and vesicular stomatitis virus envelope protein G (VSV-G) plasmids using a weight ratio of 1:0.8:0.2, as described previously[18]. Huh-7 and Huh-7.5 cells were transduced by incubation for 6 h at 37 °C with TRIPpp diluted 1:3 in complete media supplemented with 4 μg/ml polybrene and 20 mM HEPES. In some cases, transduced hepatoma cell populations were enriched using a FACSAria II high-speed flow cytometry cell sorter (BD Biosciences). For transduction of MPCC, cultures were first treated for ~20 s with 0.025% EDTA/Trypsin, before washing and overnight incubation with 1:3 diluted TRIPpp stocks.

Immunofluorescence staining and FACS analysis. For NS5A immunostaining, cells grown on glass coverslips were washed with PBS before fixation in formaldehyde (3.7% wt/vol in PBS) and incubation in blocking buffer (3% BSA, 0.2% saponin in PBS). After overnight incubation at 4 °C with monoclonal antibody 9E10 (ref. 31) (1:2,000 in blocking buffer) and 1 h incubation at 25 °C with AlexFluor-594-conjugated secondary antibody to mouse (Invitrogen, 1:1,000 in blocking buffer), cell nuclei were stained with Hoechst dye (Thermo Scientific). Coverslips were mounted using ProLong Gold Antifade reagent (Invitrogen). For IPS-1 immunostaining, cells grown on glass bottom multiwall plates (MatriCal) were washed with PBS and fixed with 2% paraformaldehyde. After incubation in blocking buffer for 30 min, and polyclonal anti-IPS-1 antibody (Cell Signaling Technology, 1:50 in blocking buffer) for 2 h, AlexaFluor-555 or AlexaFluor-488 conjugated anti-rabbit IgG secondary antibodies (Cell Signaling Technology, 1:500 in blocking buffer) were added for 1 h at 25 °C. Cells were then stained with Hoechst nuclear dye followed by application of ProLong Gold Antifade reagent. For FACS analysis, cells were harvested using AccuMax (eBioscience) and fixed using Fixation/Permeabilization buffer (BD Biosciences) for 10 min at 4 °C. Fixed cells were washed with BD Perm/Wash buffer (BD Biosciences), incubated 30 min at 25 °C with AlexaFluor-647-conjugated 9E10 antibody (1:4000 in BD Perm/Wash buffer), washed twice with BD Perm/Wash buffer and once with FACS buffer (PBS/3% FBS) before analysis using a BD LSR II flow cytometer and BD FACSDiva software. Analysis of FACS data was performed using FlowJo software.

Microscopy. Wide-field fluorescent images were captured using an Eclipse TE300 (Nikon) inverted microscope and SPOT imaging software or the Discovery-1 system and MetaXpress software (Molecular Devices). Confocal imaging of fixed samples was performed using an inverted Axiovert 200 laser scanning microscope (Zeiss). For long-term live cell imaging, cells were grown on rat-tail collagen–coated (BD Biosciences) no. 1.5 Lab-Tek II 4-chambered (Thermo Fisher Scientific) coverslips. Live cells maintained at 37 °C in imaging media were imaged using a Zeiss Axiovert 200 inverted microscope equipped with an UltraView spinning disk confocal head (Perkin-Elmer), an Orca ER-cooled CCD camera (Hamamatsu), a 20×/0.75 N.A. Plan-Apochromat objective, and an environmental chamber (Solent Scientific). Solid-state 491 and 561 nm lasers (Spectral Applied) and ET 530/50 and ET 605/70 emission filters (Chroma) were used for excitation and emission of EGFP and RFP fluorescence, respectively. Alternatively, time-lapse images were captured using an Olympus IX71 inverted microscope equipped with an Orca ER cooled CCD camera, a 20×/0.75 N.A. UPlan SApo objective and an environmental chamber. Image acquisition was performed using Metamorph (Molecular Devices) and processing was performed using ImageJ64.

30. Pietschmann, T. *et al.* Construction and characterization of infectious intragenotypic and intergenotypic hepatitis C virus chimeras. *Proc. Natl. Acad. Sci. USA* **103**, 7408–7413 (2006).
31. Lindenbach, B.D. *et al.* Complete replication of hepatitis C virus in cell culture. *Science* **309**, 623–626 (2005).
32. Lindenbach, B.D. & Rice, C.M. Trans-complementation of yellow fever virus NS1 reveals a role in early RNA replication. *J. Virol.* **71**, 9608–9617 (1997).
33. Petrakova, O. *et al.* Noncytopathic replication of Venezuelan equine encephalitis virus and eastern equine encephalitis virus replicons in mammalian cells. *J. Virol.* **79**, 7597–7608 (2005).
34. Zennou, V. *et al.* HIV-1 genome nuclear import is mediated by a central DNA flap. *Cell* **101**, 173–185 (2000).

doi:10.1038/nbt.1604

Real-time imaging of hepatitis C virus infection using a fluorescent cell-based reporter system

Christopher T. Jones, Maria Teresa Catanese, Lok Man J. Law, Salman R. Khetani, Andrew J. Syder, Alexander Ploss, Thomas S. Oh, John W. Schoggins, Margaret R. MacDonald, Sangeeta N. Bhatia, and Charles M. Rice

Supplementary material

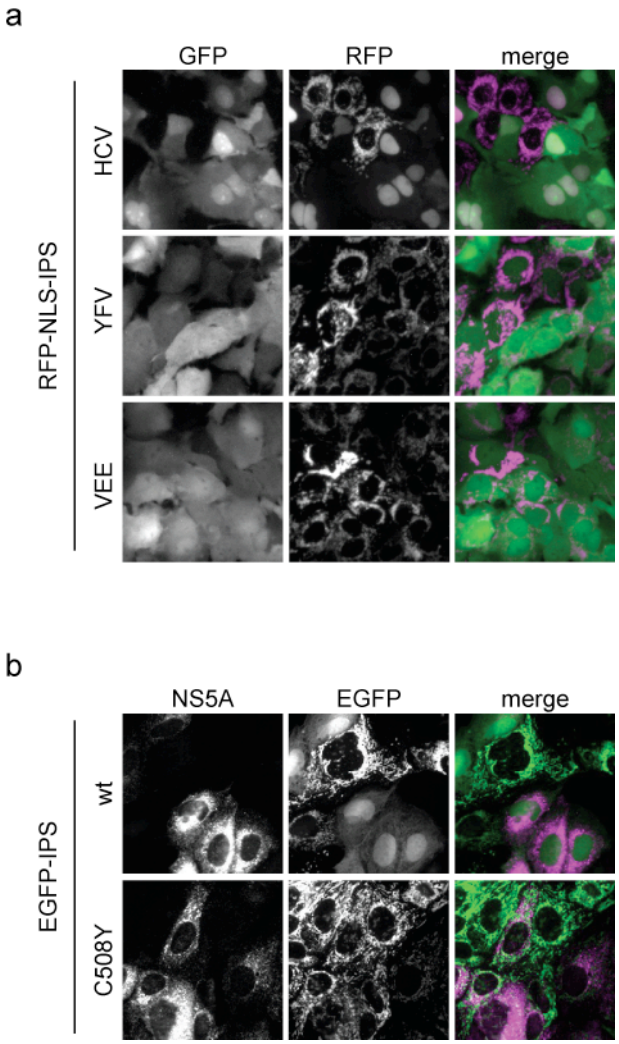

Supplementary Figure 1. HCV-specificity of the IPS-1-based reporter system (**a**) RFP-NLS-IPS relocalization is not a pan-viral phenotype. Huh-7.5 cells harboring RFP-NLS-IPS were infected with RNA viruses expressing green fluorescent proteins: an HCVcc reporter genome expressing Ypet (HCV, 48 h post infection), yellow fever virus expressing Venus (YFV, 24 h post infection), or Venezuelan equine encephalitis encoding EGFP (VEE, 8 h post infection)**.** Grayscale images show virally-encoded green fluorescence (GFP) and RFP-NLS-IPS localization (RFP). Merge images indicate an association between HCV, but not YFV or VEE, infection and nuclear RFP-IPS fluorescence. Wide-field fluorescence images of unfixed cells are shown. (**b**) EGFP-IPS relocalizes in HCV-infected cells**.** Huh-7.5 cells expressing wild type (wt) or mutant (C508Y) EGFP-IPS were infected with HCVcc virus, Jc1. Grayscale images show EGFP-IPS fluorescence (EGFP) and immunostaining for an HCV replicase protein (NS5A) in fixed cells at 48 h post-infection. Merged images show correlation of NS5A-positivity and diffuse EGFP in wt, but not C508Y, reporter cells.

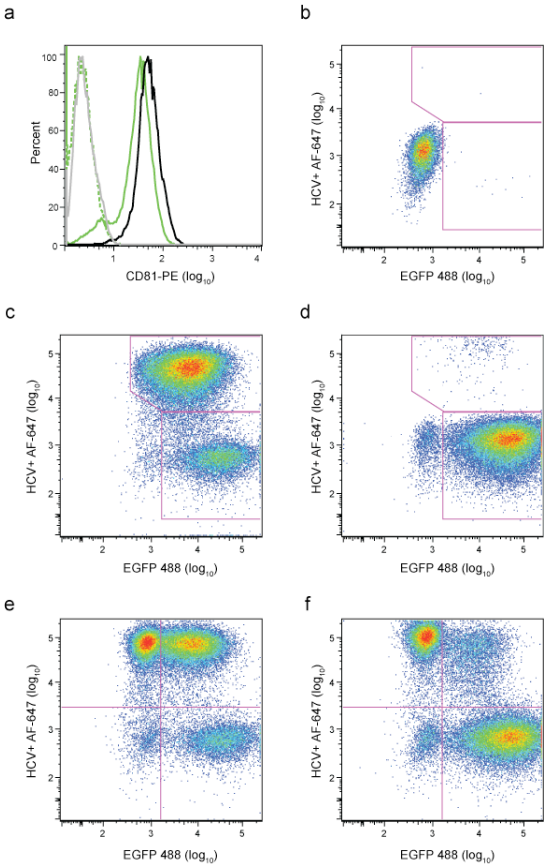

	Cultures: (% HCV+ cells)	
	Mono-	Co-
RFP-NLS-IPS	92.4	93
EGFP-IPS/IRR	78.5	79.2
EGFP-IPS/CD81$^-$	0.64	13.7

Supplementary Figure 2. FACS analysis of HCVcc-infected reporter cell mono- and co-cultures. (**a**) CD81 expression in uninfected wild type (wt) and shRNA-expressing Huh-7.5 cell lines, as detected by staining with PE-conjugated anti-CD81 antibody. Huh-7.5 cells, solid black line; EGFP-IPS/IRR cells, solid green line; EGFP-IPS/CD81$^-$ cells, dashed green line and grey line (unstained). NS5A, detected by staining with 9E10 conjugated to AlexFluor-647, and EGFP signals of uninfected Huh-7.5 cells (**b**) and J6/JFH clone 2-infected monocultures of EGFP-IPS/IRR (**c**) or EGFP-IPS/CD81$^-$ cells (**d**). NS5A and EGFP levels in co-cultures of J6/JFH clone 2-infected RFP-NLS-IPS cells with EGFP-IPS/IRR (**e**) or EGFP-IPS/CD81$^-$ (**f**) cells. Table shows percent NS5A-positive cells for each cell population in mono- or co-culture.

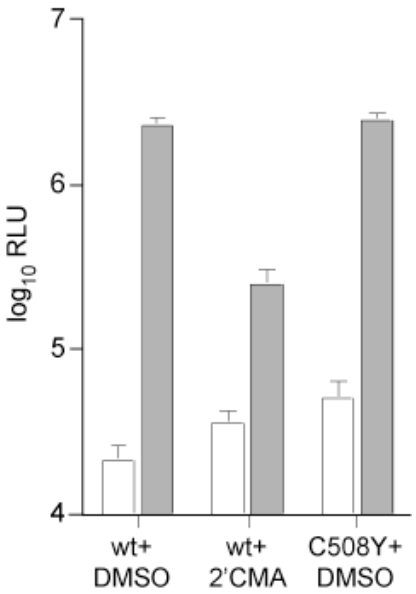

Supplementary Figure 3. Infection of primary hepatocyte MPCC. MPCC transduced with lentiviruses expressing wild type (wt) or mutant (C508Y) RFP-NLS-IPS were infected with Jc1FLAG2(p7-nsGluc2A). At 12 h post-infection virus was removed, cells were washed three times, and media was replaced with MPCC media containing DMSO or 2'CMA. Levels of secreted *Gaussia* luciferase activity were measured immediately after media replacement (white bars) and at 48 h post-infection (grey bars). Average values of three independent infections are shown; error bars represent standard error of the mean. Graph generated using Prism 4 software.

Supplementary Video 1. Time-lapse live cell imaging of HCVcc infection. Huh-7.5 cells expressing mito-EGFP and RFP-NLS-IPS were infected with Jc1FLAG2(p7-nsGluc2A) in the presence of DMSO or 2'CMA. At 5 h post infection, virus was removed and replaced with imaging media containing either DMSO (**a**) or 2'CMA (**b**). Images were captured every 30 min, starting at 6 h post-infection. In a second experiment, cells were infected for 24 h prior replacement of complete media with imaging media containing DMSO (**c**) or VX-950 (**d**). Image acquisition was initiated 0.5 h after the addition of imaging media. Images were assembled and processed using ImageJ64 software. For clarity only RFP images (displayed as grayscale) are shown.

Supplementary Video 2. Time-lapse live cell imaging of HCV-induced stress response. Huh-7 cells expressing RFP-NLS-IPS and EGFP-G3BP were infected with Jc1FLAG2(p7-nsGluc2A). At 5 h post-infection virus was removed and replaced with imaging media containing DMSO (**a** and **b**) or 2'CMA (**c**). Images were captured every 30 min, starting at 6 h post-infection. Images were assembled and processed using ImageJ64 software. RFP-NLS-IPS (left), EGFP-G3BP (middle), color merge (right).